PAPER • OPEN ACCESS

Temperature gradient-induced magnetization reversal of single ferromagnetic nanowires

To cite this article: Ann-Kathrin Michel *et al* 2017 *J. Phys. D: Appl. Phys.* **50** 494007

View the article online for updates and enhancements.

Temperature gradient-induced magnetization reversal of single ferromagnetic nanowires

Ann-Kathrin Michel[1]**, Anna Corinna Niemann**[1,2] ⓘ**, Tim Boehnert**[1,3] ⓘ**, Stephan Martens**[1]**, Josep M Montero Moreno**[1]**, Detlef Goerlitz**[1] ⓘ**, Robert Zierold**[1]**, Heiko Reith**[2]**, Victor Vega**[4]**, Victor M Prida**[4]**, Andy Thomas**[2]**, Johannes Gooth**[1,5] **and Kornelius Nielsch**[1,2,6,7]

[1] Institute of Nanostructure and Solid State Physics, Universität Hamburg, Jungiusstrasse 11 B, 20355, Hamburg, Germany
[2] Leibniz Institute for Solid State and Material Research, Helmholtzstraße 20, D-01069, Dresden, Germany
[3] INL International Iberian Nanotechnology Laboratory, Av. Mestre José Veiga, 4715-330, Braga, Portugal
[4] Depto. Física, Fac. Ciencias, Universidad de Oviedo, C/Federico García Lorca 18, E-33007, Oviedo, Spain
[5] IBM Research-Zurich, Säumerstrasse 4, 8803 Rüschlikon, Switzerland
[6] Technische Universität Dresden, Institute of Materials Science, 01062 Dresden, Germany
[7] Technische Universität Dresden, Institute of Applied Physics, 01062 Dresden, Germany

E-mail: a.niemann@ifw-dresden.de and k.nielsch@ifw-dresden.de

CrossMark

Abstract

In this study, we investigate the temperature- and temperature gradient-dependent magnetization reversal process of individual, single-domain $Co_{39}Ni_{61}$ and $Fe_{15}Ni_{85}$ ferromagnetic nanowires via the magneto-optical Kerr effect and magnetoresistance measurements. While the coercive fields (H_C) and therefore the magnetic switching fields (H_{SW}) generally decrease under isothermal conditions at elevated base temperatures (T_{base}), temperature gradients (ΔT) along the nanowires lead to an increased switching field of up to 15% for $\Delta T = 300\,K$ in $Co_{39}Ni_{61}$ nanowires. This enhancement is attributed to a stress-induced, magneto-elastic anisotropy term due to an applied temperature gradient along the nanowire that counteracts the thermally assisted magnetization reversal process. Our results demonstrate that a careful distinction between locally elevated temperatures and temperature gradients has to be made in future heat-assisted magnetic recording devices.

Keywords: magnetic nanowires, nanoelectronics, magneto-optical Kerr effect

(Some figures may appear in colour only in the online journal)

Magnetic memory devices are the workhorses of modern digital data storage [1]. The first commercial magnetic hard disk drives were introduced in 1957 by IBM [2] and held a storage capacity of $2\,kb\,in^{-2}$. Since then, tremendous progress in the

optimization of magnetic memory devices has been made to the extent that in 2014, Seagate [3] announced a device with a memory capacity of $826\,Gb\,in^{-2}$. However, the main reason for this track record is the continuous down-scaling of the geometrical single magnetic bit unit sizes, which is restricted by the superparamagnetic limit. Accordingly, reliable data storage is inhibited below a certain particle size because the thermal activation energy induces random bit flipping. Driven by the

need to overcome this limit, alternative concepts for future magnetic data storage have emerged. One of the most distinct approaches is heat-assisted magnetic recording (HAMR) [4, 5], where the shape or crystal anisotropy enhances the magnetic switching fields, H_{SW}, (and therefore the coercivity, H_C) and suppresses the superparamagnetic limit, while a heating laser pulse that decreases H_C for a short period of time is used to allow for a magnetic bit writing process. In fact, for highly anisotropic FePt HAMR devices, a data storage areal density of 1.4 Tb in^{-2} has recently been demonstrated in a laboratory environment [6].

Parallel to the efforts to incorporate heat pulses into magnetic memory devices, the research field of spin-caloritronics [7] evolved, seeking a fundamental understanding of the interplay between charge, spin and heat. While the HAMR technique basically relies on induced magnetic switching at elevated temperature pulses, temperature gradients were also found to generate numerous spin-caloritronic effects. Currently, classical thermoelectric effects in ferromagnetic materials systems are quite well-established. The so-called spin-dependent Seebeck effect has been observed in anisotropic magnetoresistance (MR) [8, 9], giant MR [10, 11] and tunnel MR [12, 13] regimes. The spin-Seebeck effect (SSE) [14, 15], which describes the generation of a pure spin current due to a temperature gradient in a ferromagnetic material, is currently under intense investigation. Furthermore, the thermal spin transfer torque (TSTT) has attracted much attention because the effect on the magnetic switching behavior of magnetic tunnel junctions is three orders of magnitude larger than its spintronic equivalent effect (the spin transfer torque) can account for, due to charge currents generated by the spin-dependent Seebeck effect [16].

In this study, we directly compare the influence of the base temperature, T_{base}, and temperature gradients, ΔT, on the magnetization reversal of ferromagnetic nanostructures. Therefore, magneto-optical Kerr (MOKE) measurements and MR measurements were performed on individual $Co_{39}Ni_{61}$ and $Fe_{15}Ni_{85}$ nanowires under an externally applied magnetic field, $\mu_0 H$, at different ΔT and T_{base} values. We show that H_{SW} generally decreases with increasing T_{base}, while the magnetic switching field of $Co_{39}Ni_{61}$ nanowires increases for increasing ΔT. We attribute this increase in H_{SW} for increasing ΔT to a stress-induced enhancement of the magneto-elastic anisotropy and develop a simple approach to estimate the H_C values as a function of the applied ΔT.

Cylindrical ferromagnetic nanowires with an average diameter of 150 nm and lengths of up to 30 μm were grown by template-assisted electrodeposition into self-ordered, nanoporous alumina (AAO) membranes [17]. Two types of soft magnetic alloy nanowires—$Fe_{15}Ni_{85}$ and $Co_{39}Ni_{61}$—were synthesized according to previously followed procedures from Salem *et al* [18] and Vega *et al* [19], respectively. Prior to electrodeposition, the internal walls of the alumina membranes had been coated with an approx. 10 nm thick layer of SiO_2 by atomic layer deposition [20, 21]. The SiO_2 cover layer protects the nanowires from oxidation and additionally supplies mechanical stability when the nanowires are suspended in ethanol after being released from the AAO template by selective chemical etching.

Two types of micro-devices (A and B) were designed to measure the optical and electrical properties of the individual nanowires (figures 1(a) and 2(a), respectively). Therefore, the suspended nanowire/ethanol solution was applied dropwise to a 150 μm thick quartz substrate, and the micro-devices were defined by laser beam lithography followed by a metallization process [9].

Micro-device A consists of two Ti/Pt lines—one at each end of the nanowire—which are not in electrical contact with the nanowire (figure 1(a)) and which have been simultaneously used as heater lines and as resistive thermometers. DC currents up to 10 mA generated temperature gradients via Joule heating in the heater line, which led to temperatures up to 680 K at the hot thermometer and 380 K at the cold thermometer. Hence, temperature gradients, ΔT, up to 300 K were generated along the nanowire (figure 1(b)). We note that the actual temperature difference along the nanowire is slightly below the measured temperature difference, because the nanowire is about 1 μm shorter than the distance between the thermometers.

Micro-device A was used to measure the coercive fields of $Co_{39}Ni_{61}$ and $Fe_{15}Ni_{85}$ nanowires as a function of the applied temperature gradients via the longitudinal MOKE [22]. A NanoMOKE™2 from *Durham Magneto Optics* equipped with an (45°) incidence continuous wave-laser light with a power output of 1.9 mW and with an in-plane focused spot size of approximately 3 μm was used. Alternating magnetic fields up to ± 0.08 T could be applied with a quadrupole magnet in the plane of incidental beam of light and thus parallel to the nanowire axis, as described in detail by Vega *et al* [19]. With a distance of approx. 500 nm between the nanowire and the heater line, the estimated maximum Oersted fields induced by the heater lines to the nanowire were in the order of 10^{-4} T and could be excluded from having an impact on the magnetization reversal of the nanowire. Furthermore, the temperature rise due to the incidental laser beam could be neglected in this study due to an estimated heating of less than 1 K. The recorded hysteresis loops show no deviation whether the laser spot was focused on the wire's edges or on its center, and the square-like MOKE hysteresis curves exhibited symmetric Barkhausen jumps for $Fe_{15}Ni_{85}$ and the $Co_{39}Ni_{61}$ nanowires. In figure 1(c), the hysteresis loop of the $Co_{39}Ni_{61}$ nanowire measured at $T_{base} = 300$ K and for $\Delta T = 0$ K was exemplarily given with a coercive field of 424 G. Due to the low signal-to-noise ratio, it became necessary to successively average data over several hundred single shot hysteresis loops.

Micro-device B (figure 2(a)) corresponded with the typical experimental setup [9, 23] for measuring the thermopower, S ($S = U_{th}/\Delta T$, with U_{th} being the thermo-voltage induced by the temperature gradient ΔT), of nanowires. The microdevice consisted of one resistive heater line (yellow) and two resistive thermometers (red and blue for the hot and cold thermometer, respectively). For the thermoelectric characterization, applied DC currents flowing through the resistive heater line generated a temperature gradient along the nanowire. Employing both resistive thermometers, ΔT was determined, and U_{th} was measured along the nanowire. For a general characterization of our sample we determined the resistivity, ρ, and S of the nanowires. Resistance measurements were conducted
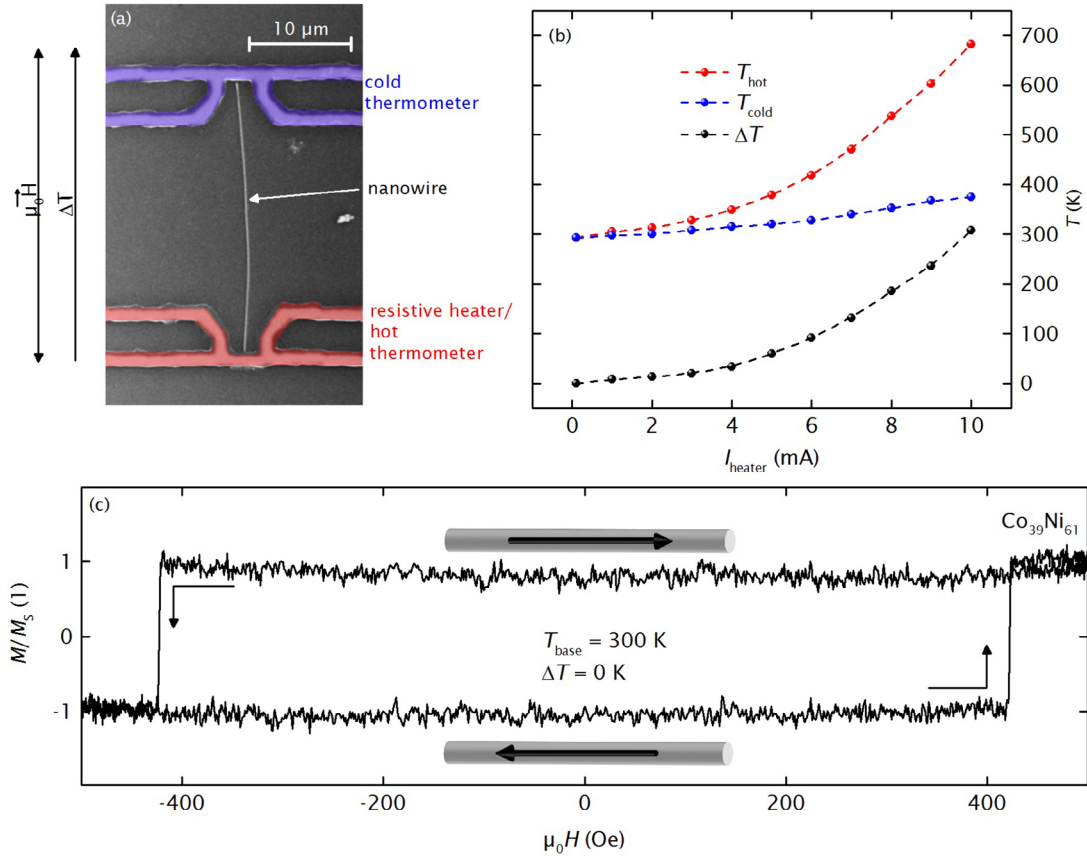
Figure 1. MOKE measurements: (a) the experimental setup for the MOKE measurements is sketched on a scanning electron microscopy image of the utilized micro-device A. The nanowire is surrounded by two Ti/Pt lines, which are not in electrical contact with the nanowire and serve as both Joule heaters and resistive thermometers, simultaneously. An external magnetic field was applied parallel to the nanowire axis, and a linear polarized laser beam was focused on the nanowire for longitudinal MOKE measurements as a function of the applied temperature gradient. (b) The temperatures at both resistive thermometers T_{hot} and T_{cold} and the resulting temperature difference ΔT are shown as a function of the DC heating current I_{heater}, which is supplied to the Joule heater. (c) Hysteresis loop of a $Co_{39}Ni_{61}$ nanowire measured at room temperature and without an applied temperature gradient. The nanowire (gray rod) and its magnetization (black arrow) are sketched for the upper and lower branch of the hysteresis curve.

in a four-point measurement geometry, for which we used the hot and cold thermometers (figure 2(a)) as the electrodes. We observed metallic $\rho(T)$-curves for both material systems with room temperature values of $\rho(Fe_{15}Ni_{85}) = 34.5\ \mu\Omega$ cm and $\rho(Co_{39}Ni_{61}) = 19.7\ \mu\Omega$ cm, which are higher than the corresponding bulk literature values of $\rho(Fe_{15}Ni_{85},$ bulk$) = 14\ \mu\Omega$ cm and $\rho(Co_{39}Ni_{61},$ bulk$) = 11\ \mu\Omega$ cm [24]. These enhanced resistivity values of the nanostructures compared to bulk materials are commonly observed and attributed to the nanocrystalline nature of the electrodeposited nanowires [25]. The thermopower of $Fe_{15}Ni_{85}$ and $Co_{39}Ni_{61}$ nanowires is displayed as a function of T_{base} in figure 2(b). At 300 K, we measured $S(Fe_{15}Ni_{85}) = -32\ \mu V\ K^{-1}$ and $S(Co_{39}Ni_{61}) = -26\ \mu V\ K^{-1}$. For comparison, Co and Ni bulk samples have a thermopower [26, 27] of $S(Co) = -30, 8\ \mu V\ K^{-1}$ and $S(Ni) = -18, 4\ \mu V\ K^{-1}$, respectively while the Fe–Ni bulk samples [28] showed a room temperature thermopower of $S(Fe–Ni) = -35\ \mu V\ K^{-1}$.

Additionally, micro-device B was also used to determine the temperature-dependent coercive fields of $Co_{39}Ni_{61}$ and $Fe_{15}Ni_{85}$ nanowires. In a probe station setup, we therefore performed MR measurements with the externally applied

magnetic field up to 0.5 T parallel to the nanowire axis and in the temperature range from 290 K to 350 K. Distinct resistance jumps on the order of 50 mΩ can be observed at the switching field values as exemplarily shown for a $Fe_{15}Ni_{85}$ nanowire with a coercive field of 178 G (figure 2(c)).

For $\Delta T = 0$ K, H_C for $Fe_{15}Ni_{85}$ as well as $Co_{39}Ni_{61}$ nanowires decreased in the MR measurements with increasing T_{base} (figure 3(a)). The reduction of the temperature normalized coercive field, taken as the coercivity measured at any temperature referred to the value at T = 300 K, $(H_C(T)/H_C(300\,K))$ for $Fe_{15}Ni_{85}$ nanowires (4% from 300 K to 350 K) is slightly steeper than for the one of $Co_{39}Ni_{61}$ nanowires (1% from 300 K to 350 K). Such decrease in H_C value with increasing T was a consequence of the thermally assisted switching process—the basic concept of HAMR devices.

In a next step, H_C of the $Co_{39}Ni_{61}$ and $Fe_{15}Ni_{85}$ nanowires as a function of ΔT was investigated in the NanoMOKE setup. Longitudinal MOKE hysteresis loops for $Co_{39}Ni_{61}$ and $Fe_{15}Ni_{85}$ nanowires were measured with applied ΔT between 0 K and 300 K along the nanowire axis, and the applied magnetic field $\mu_0 H$ parallel to the nanowire axis as shown in figure 3(b). For $Fe_{15}Ni_{85}$ nanowires, we observed a decrease
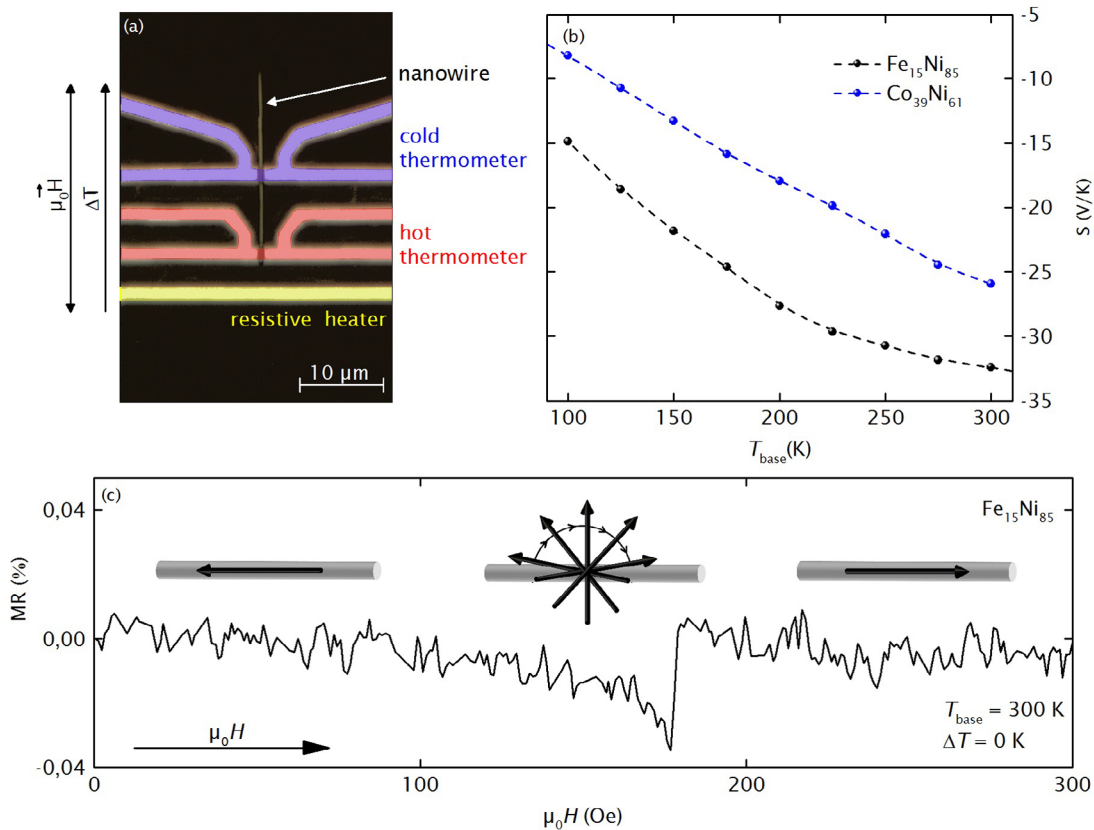
Figure 2. MR and thermopower measurements: (a) micro-device B for measuring the thermopower, S, consists of one heater line (yellow) and two resistive thermometers (red and blue) that are in electrical contact with the nanowire. Additionally, MR measurements were performed on this device with an external magnetic field, $\mu_0 H$, parallel to the nanowire axis. (b) S, as a function of the temperature, T, for $Co_{39}Ni_{61}$ and $Fe_{15}Ni_{85}$ nanowires. (c) MR (MR = $(R_H - R_0)/R_0$) as a function of $\mu_0 H$ for $Fe_{15}Ni_{85}$ nanowires, measured at room temperature and without applied temperature gradients. At the coercive field, H_C, a jump in the MR signal can be observed. The nanowire (gray rod) and its magnetization (black arrow) are sketched before, during and after the magnetization reversal process at the corresponding field values $\mu_0 H$.

of H_C with increasing ΔT of 4% for $\Delta T = 100\,K$. In contrast, we surprisingly found an increasing H_C for increasing ΔT for the $Co_{39}Ni_{61}$ nanowires. This observation remained valid even when we changed the material of the micro-device from Pt to Au to exclude any influence by the electrical contact material (figure 3(b)). Therefore, we conclude that the increase in H_C with increasing ΔT has an intrinsic origin that counteracts the average temperature-assisted switching mechanism.

To explain the unexpected $H_C(\Delta T)$ dependence of the $Co_{39}Ni_{61}$ nanowires, we will discuss possible origins in the following, whereas we start with considering stress-induced changes on the magnetic switching mechanism.

Our first hypothesis is an axial stress-induced enhancement of H_C due to an increasing ΔT along the nanowire axis. To establish an easy, quantitative model for $H_C(\Delta T)$, we start with [29]

$$H_C = \frac{2K_{eff}}{\mu_0 M_s}|\cos(\theta)| \qquad (1)$$

with the vacuum permeability μ_0, the saturation magnetization M_S, the angle θ between external magnetic field $\mu_0 H$ and the magnetization vector, and the effective anisotropy constant K_{eff} of the nanowires, which is given by $K_{eff} \approx K_{shape} + K_{me}$, with the shape anisotropy constant K_{shape} and

the magneto-elastic anisotropy constant K_{me}. Note that we neglect the magneto-crystalline anisotropy in our nanowire because it is rather small regarding the magneto-crystalline anisotropy constants [30, 31] of 5 kJ m^{-3} and 7.5 kJ m^{-3} for $Co_{39}Ni_{61}$ and $Fe_{15}Ni_{85}$, respectively. Due to their high aspect ratio, the magnetization of the nanowires and therefore their magnetization reversal in the relaxed state without induced stress are dominated by shape anisotropy. The shape anisotropy constant of an infinitely long wire is given by [32]

$$K_{shape} = \frac{1}{4}\mu_0 M_s^2. \qquad (2)$$

Using the literature values [32, 33] of the saturation magnetization $M_s(Co_{50}Ni_{50}) = 1060$ kA m^{-1} and $M_s(Fe_{20}Ni_{80}) = 795$ kA m^{-1} a shape anisotropy constant of $K_{shape}(Co_{39}Ni_{61}) \approx 350$ kJ m^{-3} and of $K_{shape}(Fe_{15}Ni_{85}) \approx 200$ kJ m^{-3} is obtained. The magneto-elastic anisotropy constant is given by [34]

$$K_{me} = \frac{3}{2}\lambda_{me}\sigma. \qquad (3)$$

λ_{me} is the magnetostriction coefficient, and σ is the axial stress given by $\sigma = \alpha_{Co/Ni/Fe}Y\Delta T$. Here, Y is the Young's modulus ($Y_{Ni,Co,Fe} \approx 209$ GJ m^{-3}), and $\alpha_{Co/Ni/Fe}$ reflects the thermal expansion coefficients [35] $\alpha_{Co} = 13.0 \cdot 10^{-6}$ K^{-1},

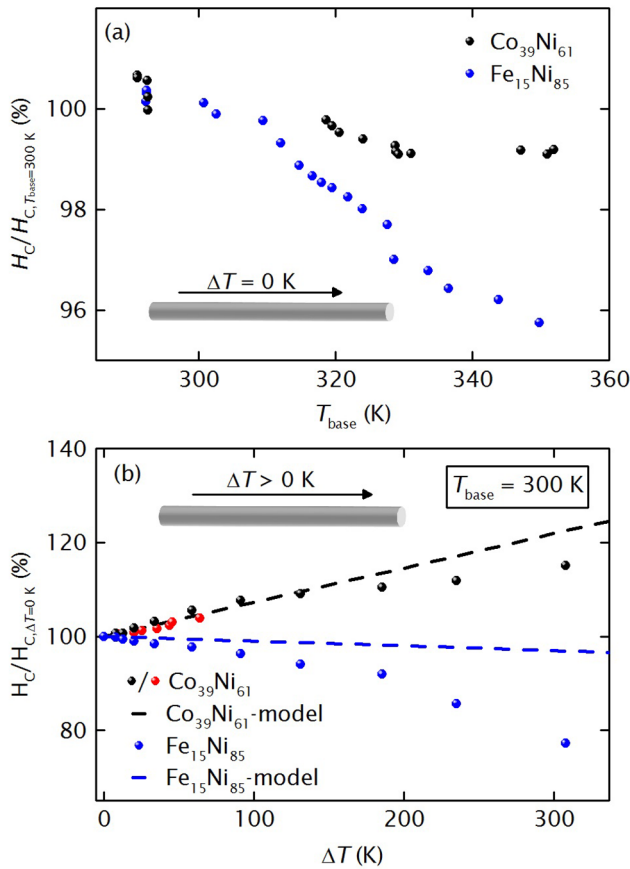**Figure 3.** Temperature- and temperature gradient-dependent coercive fields of $Co_{39}Ni_{61}$ and $Fe_{15}Ni_{85}$ nanowires: (a) temperature normalized coercive fields $H_C/H_C(T_{base} = 300\,K)$ for $Co_{39}Ni_{61}$ and $Fe_{15}Ni_{85}$ nanowires as a function of T_{base} and with $\Delta T = 0\,K$. (b) $H_C/H_C(\Delta T = 0\,K)$ for $Co_{39}Ni_{61}$ and $Fe_{15}Ni_{85}$ nanowires as a function of the applied ΔT at $T_{base} = 300\,K$. Black dots correspond to a $Co_{39}Ni_{61}$ nanowire contacted with platinum leads, blue dots correspond to a Fe15Ni85 nanowire contacted with platinum leads, and the red dots correspond to a $Co_{39}Ni_{61}$ nanowire contacted with gold leads.

$\alpha_{Ni} = 13.4 \cdot 10^{-6}\,K^{-1}$, and $\alpha_{Fe} = 11.8 \cdot 10^{-6}\,K^{-1}$ of Co, Ni and Fe at 300 K, respectively. Thus, a temperature gradient of 300 K along the nanowire leads to a stress of about $\sigma(\Delta T = 300\,K) \approx 800\,MJ\,m^{-3}$ along the nanowire axis in all investigated material systems. Now, for $\Delta T = 300\,K$ the relatively low magnetostriction coefficient [36] of the $Fe_{15}Ni_{85}$ ($\lambda_{me} = -5 \times 10^{-6}$) leads to a minor contribution of $K_{me} = -6\,kJ\,m^{-3}$ even for the highest thermal stress, such that $K_{eff} \approx K_{shape}$. For the $Co_{39}Ni_{61}$ system with the ten-times higher magnetostriction coefficient [37] $\lambda_{me} = 65 \times 10^{-6}$, however, we obtain $K_{me} = 78\,kJ\,m^{-3}$ for $\Delta T = 300\,K$, which is one order of magnitude higher than $K_{me}(Fe_{15}Ni_{85})$ and provides a significant contribution to the magnetic configuration in the nanowire. In fact, for $\Delta T = 300\,K$ and using equation (1), we obtain a relative change in the coercive field of $\frac{H_C(\Delta T = 300\,K)}{H_C(\Delta T = 0\,K)} = 1.22$ for the $Co_{39}Ni_{61}$ nanowires as indicated by the dashed line in figure 3(b). We find a very good agreement between our estimation and the experimental data for $\Delta T < 200\,K$. At higher ΔT, the measured $H_C(\Delta T)$ deviates to a less steep increase than that predicted by our model, which

we attribute to the heat-assisted magnetization reversal process due to the elevated average temperature of the nanowire caused by the high applied ΔT. For the $Co_{39}Ni_{61}$, the deviation between the measured $H_C(\Delta T)$ and the calculated $H_C(\Delta T)$ is 7% at $\Delta T = 300\,K$. Performing the same estimation of $H_C(\Delta T)$ for the $Fe_{15}Ni_{85}$ nanowire only yields a stress-induced decrease of the normalized H_C to 0.97 at $\Delta T = 300\,K$, as shown by the blue dotted line in figure 3(b). As a result, the heat-assisted switching process determines $H_C(\Delta T)$ for the $Fe_{15}Ni_{85}$ nanowires, and the measured $H_C(\Delta T)$ is significantly smaller than the estimated values regarding the stress-induced magneto-elastic anisotropy component, which leads to a difference of 20% between the measured $H_C(\Delta T)$ and the normalized $H_C(\Delta T)$ estimated with our model at $\Delta T = 300\,K$. Extrapolating the $H_C(T_{base})$ (see figure 3(a)) of the nanowires to $T_{base} = 600\,K$ ($\Delta T = 300\,K$) gives a decrease of $H_C(T_{base})$ of 5% for the $Co_{39}Ni_{61}$ nanowire and 20% for the $Fe_{15}Ni_{85}$ nanowire, which is for both material systems in good agreement with the difference between measured and calculated values of $H_C(\Delta T)$ at $\Delta T = 300\,K$.

Increasing H_C with increasing ΔT for the $Co_{39}Ni_{61}$ nanowires due to increasing radial stress-induced by the nanowire-core/SiO_2-shell is unlikely because radial stress is also present for the measurements with increasing base temperature, where we observed a decreasing H_C for increasing T_{base}.

To our knowledge, saturation magnetostriction $\lambda_S(\sigma, T)$, affecting the hysteretic behavior of ferromagnetic nanowires has so far only been reported for nanowire arrays within the template, which are exposed to uniform temperature enhancements. Kumar *et al* [34] observed increasing H_C with increasing T for Ni nanowires in an AAO template with a thick Al backside. Due to the different thermal expansion coefficients of Ni, AAO and Al, they calculated magneto-elastic anisotropy constants between $-42\,kJ\,m^{-3}$ and $-96\,kJ\,m^{-3}$. Silva *et al* [38] investigated Co nanowires in AAO templates and found that longer nanowire segments experience a stronger thermal expansion and therefore more stress in the AAO templates for decreasing T than shorter nanowires, which leads to change in the easy magnetization axis from parallel to perpendicular direction to the nanowire axis that occurs nearer to the electrodeposition temperature of 300 K for longer Co nanowire than for shorter Co segments. Pirota *et al* [39] intensified this study on Ni nanowires in AAO templates and calculated (thermal) induced stresses between $-170\,kJ\,m^{-3}$ for short ($l = 0.5\,\mu m$) nanowires and $-780\,kJ\,m^{-3}$ for longer ($l = 2.2\,\mu m$) segments.

Another effect that might have a noticeable influence on the switching mechanism of magnetic nanowires under a temperature gradient is the TSTT. It has been recently demonstrated that the TSTT has a much higher effect on the magnetization reversal characteristics of tunnel MR structures than the STT due to a spin-dependent Seebeck effect accounting for [16]. One underlying mechanism for this observation in our samples geometry could be a pure spin current due to the longitudinal SSE [15] that can have a stabilizing or destabilizing effect on the magnetization of the nanowire and therefore decreases or increases the coercivity H_C. Overall, we believe that the interplay of the stress-induced contributions of the

J. Phys. D: Appl. Phys. **50** (2017) 494007

A-K Michel *et al*

magneto-elastic anisotropy and an intrinsic thermally assisted switching mechanism described in this work fits the data accurately. Thus, we conclude that no major influences of the TSTT and the longitudinal SSE are observed in these samples.

In summary, we synthesized $Co_{39}Ni_{61}$ and $Fe_{15}Ni_{85}$ nanowires to investigate temperature- and temperature-gradient dependent magnetization reversal process of ferromagnetic nanostructures. Performing MR measurements, we found that the magnetic switching fields (and therefore their coercivities) decreased with increasing the base temperature for both $Co_{39}Ni_{61}$ and $Fe_{15}Ni_{85}$ nanowires. MOKE measurements with applied temperature gradients at room temperature showed a decrease in the coercive field values for $Fe_{15}Ni_{85}$ nanowires while H_C increases up to 5% per 100 K for $Co_{39}Ni_{61}$ nanowires. We attribute this increase in H_C for $Co_{39}Ni_{61}$ nanowires to a stress-induced enhancement in the magneto-elastic anisotropy contribution to the effective anisotropy due to an applied temperature gradient, and we were able to fit the measured $H_C(\Delta T)$ increase with a simple model. Our results highlight the quite distinct effects of elevated temperatures and applied temperature gradients on the switching fields and therefore on the magnetization reversal mechanisms of ferromagnetic nanostructures and reveal the challenges of future heat-assisted, magnetic recording device design.

Acknowledgments

ORCID iDs

Anna Corinna Niemann ● https://orcid.org/0000-0003-2996-7808
Tim Boehnert ● https://orcid.org/0000-0002-2659-1481
Detlef Goerlitz ● https://orcid.org/0000-0002-3496-5519

References

[1] Tehrani S, Slaughter J M, Chen E, Durlam M and Shi J 1999 *IEEE Trans. Magn.* **35** 2814–9
[2] Harker J M, Brede D W, Pattison R E, Santana G R and Taft L G 1981 *IBM J. Res. Dev.* **25** 677–90
[3] *Seagate Product Manual* Dec 2013 publication no: 100743772, rev A
[4] Rausch T, Gage E and Dykes J 2015 *Springer Proc. Phys.* **159** 200–2
[5] Rottmayer R E *et al* 2006 Heat-assisted magnetic recording *IEEE Trans. Magn.* **42** 2417–21
[6] Ju G *et al* 2015 *IEEE Trans. Magn.* **51** 11
[7] Bauer G E W, Saitoh E and van Wees B J 2012 *Nat. Mater.* **11** 391–9
[8] Avery A D, Pufall M R and Zink B L 2012 *Phys. Rev.* B **86** 1–5
[9] Böhnert T, Vega V, Michel A-K, Prida V M and Nielsch K 2013 *Appl. Phys. Lett.* **103** 092407
[10] Shi J, Parkin S S P, Xing L and Salamon M B 1993 *J. Magn. Magn. Mater.* **125** 251–6
[11] Böhnert T *et al* 2014 *Phys. Rev.* B **90** 165416
[12] Yuasa S, Nagahama T, Fukushima A, Suzuki Y and Ando K 2004 *Nat. Mater.* **3** 868–71
[13] Böhnert T, Serrano-Guisan S, Paz E, Lacoste B and Ferreira R 2017 *J. Phys.: Condens. Matter.* **29** 185303
[14] Uchida K, Takahashi S, Harii K, Ieda J, Koshibae W, Ando K, Maekawa S and Saitoh E 2008 *Nature* **455** 778–81
[15] Meier D *et al* 2015 *Nat. Commun.* **6** 8211
[16] Pushp A, Phung T, Rettner C, Hughes B P, Yang S-H and Parkin S S P 2015 *Proc. Natl Acad. Sci. USA* **112** 6585–90
[17] Nielsch K, Choi J, Schwirn K, Wehrspohn R B and Gösele U 2002 *Nano Lett.* **2** 677–80
[18] Salem M S, Sergelius P, Zierold R, Montero Moreno J M, Görlitz D and Nielsch K 2012 *J. Mater. Chem.* **22** 8549
[19] Vega V, Böhnert T, Martens S, Waleczek M, Montero-Moreno J M, Görlitz D, Prida V M and Nilesch K 2012 *Nanotechnology* **23** 465709
[20] Bachmann J, Zierold R, Chong Y T, Hauert R, Sturm C, Schmidt-Grund R, Rheinländer B, Grundmann M, Gösele U and Nielsch K 2008 *Angew. Chem., Int. Ed. Engl.* **47** 6177–9
[21] Lee J, Farhangfar S, Yang R, Schulz R, Alexe M, Gösele U, Lee J and Nielsch K 2009 *J. Mater. Chem.* **19** 7050
[22] Allwood D A, Gang X, Cooke M D and Cowburn R P 2003 *J. Phys. D.: Appl. Phys.* **36** 2175–82
[23] Shapira E, Tsukernik A and Selzer Y 2007 *Nanotechnology* **18** 485703
[24] McGuire T R and Potter R I 1975 *IEEE Trans. Magn.* **11** 4
[25] Srivastav A K and Shekhar R 2014 *J. Magn. Magn. Mater.* **349** 21–6
[26] Laubitz M J and Matsumura T 1973 *Can. J. Phys.* **51** 12
[27] Laubitz M J and Matsumura T 1976 *Can. J. Phys.* **54** 1
[28] Ho C Y, Chi T C, Bogaard R H, Havill T N and James H M 1983 *Thermal Conductivity* vol 17 ed J G Hust (New York: Plenum Press)
[29] Sánchez-Barriga J, Lucas M, Radu F, Martin E, Multigner M, Marin P, Hernando A and Rivero G 2009 *Phys. Rev.* B **80** 1–8
[30] Vivas L G, Vazquez M, Escrig J, Allende S, Altbir D, Leitao D C and Araujo J P 2012 *Phys. Rev.* B **85** 1–8
[31] Yin L F *et al* 2006 *Phys. Rev. Lett.* **97** 1–4
[32] Tannous C and Gieraltowski J 2006 *Eur. J. Phys.* **29** 475–7
[33] Van Drent W P, Bijker M D and Lodder J C 1996 *J. Magn. Magn. Mater.* **156** 309–10
[34] Kumar A, Fähler S, Schlörb H, Leistner K and Schultz L 2006 *Phys. Rev.* B **73** 1–5
[35] Nix F C and MacNair D 1941 *Phys. Rev.* **60** 597–605
[36] Bozorth R M and Walker J G 1953 *Phys. Rev.* **89** 624–62
[37] Hall R C 1959 *J. Appl. Phys.* **30** 816–9
[38] Silva E L, Nunes W C, Knobel M, Denardin J C, Zanchet D, Pirota K, Navas D and Vázquez M 2006 *Physica* B **384** 22–4
[39] Pirota K R, Silva E L, Zanchet D, Navas D, Vázquez M, Hernández-Vélez M and Knobel M 2007 *Phys. Rev.* B **76** 233410